

Investigation on Closed-loop Fiber Optic Gyroscope Structure and Operation

Rohollah Mazrae Khoshki¹ and Prof. Submarian Ganesan²

^{1,2}Oakland University, Electrical and Computer Engineering Dep.
rmazraek@oakland.edu, ganesan@oakland.edu

Abstract

In this paper, I reviewed comprehensively the structure and operation of closed-loop IFOGs, Feedback Erbium-doped fiber amplifier (EFDA) FOGs, called FE-FOG. The procedure of finding the Sagnac shift for closed-loop IFOG has been studied. The signal processing in the closed-loop IFOG was simulated using PSCAD software. In the closed-loop IFOG, the phase shift was derived through frequent use of Sagnac loop. The output signal is injected in the input again as feedback. The shift phase between clockwise and counterclockwise waves in each complete route, including primary and feedback route, is identified as Sagnac shift phase. According to Sagnac shift phase we could determine angular rotation rate.

Keywords: Interferometric Fiber Optic Gyroscope (IFOG), Feedback Erbium-doped fiber amplifier FOG (FE-FOG), Erbium-doped fiber amplifier (EFDA), PSCAD, Sagnac shift

1. Introduction

Gyroscope is a sensor which determines the rotation rate and direction. Inertial guidance and navigation systems are known to be very useful for aircrafts, land vehicles and robots for many years, in past they make use of mechanical gyroscope but today's FOG (Fiber Optic Gyroscope) is used for measurement of the rotation based on Sagnac Effect [1]. Two types of FOG are used: first the interferometric FOG (I-FOG) in which a low coherence light source is used and second the resonance FOG (R-FOG). In the R-FOG the differences of resonance frequency caused by Sagnac effect is utilized for measuring the rotation. Therefore even a short length of optical fiber is sufficient for the measurement. R-FOG needs a coherent light source for which such effects like Kerr effect and reflective optic phenomenon must be considered. The FOG converts the Sagnac phase shift into a beam frequency between the clockwise and counterclockwise of laser modes. As an example requirement of the precision of rotation measurement for spacecraft navigation lies between $0.01^{\circ}/hr$ to $0.001^{\circ}/hr$.

The principle of operation of a typical fiber gyro is based on a phase modulation in both directions of an optical fiber loop, as if it acts as a delay line. The modulation frequency, $f_p = \frac{1}{2\tau}$, matches the half period of the transit time τ . Such a modulation

scheme provides a sinusoidal response with a stable bias. However this response is nonlinear and the rotation rate proportional to the returning power is not perfectly stable.

Ring laser gyroscope (RLG) consists of a ring laser having two counter-propagating modes over the same path in order to detect rotation. It works based on Sagnac shift effect and requires high vacuum and precision mirror technology, which makes this technique very expensive [2]. The physical principal of RLG operation is analogous to the Doppler Effect, but it involves determination of the phase shift between two counter-propagating light beams in an evacuated mirrored cavity [3]. To address this drawback, interferometric fiber optic gyro (IFOG) is employed whose function resembles RLG,

notwithstanding the fact that, in IFOG, the same effect is obtained in a fiber coil with the elimination of the high voltage and high vacuum, which results in a low-cost inertial rotation sensor [2 and 3]. In addition, IFOGs are abstracted in miniature devices; all-solid state with a limited number of components, therefore lower cost.

In terms of light source, RLG requires an external narrow band gas laser with its active gain medium which is an integral part of the sensing cavity, whereas IFOG works with an external broadband light source [4]. Path length measurement in RLG is performed by measuring the difference of resonant frequencies between two cavities. Despite, IFOG rotation rate sensing is achieved through a direct measurement (open loop) or nulling (close loop) of the optical phase difference due to the rotation-induced Sagnac phase shift [5].

According to the fact that high precision gyro is not always required, e.g. in land automotive vehicle an IFOG with the accuracy between 10 to 200deg/hr is sufficient [6], and also regarding to the least requirements with the most flexibility in the design of IFOG, the improvement of this sensor becomes more sensible. Therefore in this paper I used EF-IFOG that will be explained in detail in next section.

2. Principle of EF-IFOG Operation

EF-FOG work by frequent utilize of sagnact loop, in this manner output signal re-inputted as feedback. It performs like R-FOG but without high length coherence light source and never use the resonance effect. FE-FOG in comparison with Open-loop I-FOG has high sensibility and wide dynamic range [7].

A light source with a coherence length much shorter than the coil length allows only the wave pairs that have circulated the same number of times in the loop to interfere with each other and to produce an output related to the rotation-induced nonreciprocal phase shift. The resultant optical response is essentially the sum of all the optical responses of a series of conventional Sagnac Interferometric fiber-optic gyroscopes with their effective loop length in multiples of a single coil's length. The multiple-trip interference and the associated intensity summation produces a response resembling a resonance phenomenon, with the strength and sharpness of the resonance increasing with the number of interfering light waves. The proposed gyro has different from a resonant fiber-optic gyro (R-FOG) because it uses a low coherent light source. The low coherent source minimizes not only errors from Rayleigh back scattering, but also bias errors caused by the optical Kerr effect. This could not possibly be done in an R-FOG because of high coherent light source.

If the modulation frequency of phase modulator in sagnact loop consists of whole loop time delay, the output signal in IFOG will be in pulse shape; therefore, when rotation occurs in the system, the location of output peak pulse shifts by sagnact effect. Precision of measurement depends on sharpness of the output pulses. Sharpness of output pulse is determined by the phase modulation depth and EFDA gain [8].

Miniature fiber optic gyros have also been manufactured with all solid-state optical devices for precise measurements of mechanical rotation based on the sagnac principle.

Open-loop IFOG is a simple configuration of the IFOG. Closed-loop IFOG performs similar to the resonance FOG (R-FOG), both based on Sagnac effect, although used for different tasks.

3. Rotation Equation

When the optical ring is rotated with a tangential velocity v , the beam rotating with the ring will have an optical path longer than the counter-rotating beam by a distance ΔL given by:

$$\Delta L = \frac{4\pi R v}{c} \quad (1)$$

Where, R is the ring radius and c is the speed of light in the vacuum. For a monochromatic light of wavelength λ , this change in optical path length results in the Sagnac phase difference, which is given by Equation (2).

$$\Delta \phi = \frac{2\pi}{\lambda} \Delta L = \frac{8\pi^2 R v}{\lambda c} \quad (2)$$

The phase difference between two beams, after passing the ring with the area A and rotating with an angular velocity Ω , generates a phase difference which is given by:

$$\Delta \phi = \frac{8\pi A \Omega}{\lambda c} \quad (3)$$

It is important to note that, the resultant phase shift is independent of the medium and of the exact shape of the loop. This compliant property of the IFOG is an advantage when it is required to design it to fit the volume constrains in the specific applications. However, the resultant phase shift can be increased by additional loops (turns of fiber) i.e. if it is wound N turns of the fiber coil. The resultant phase shift becomes [9]:

$$\Delta \phi = \frac{8\pi A \Omega N}{\lambda c} \quad (4)$$

Alternatively, we can express the resultant phase shift in terms of coil diameter and fiber length by noting that:

$$A = \frac{\pi D^2}{4} \quad (5)$$

And,

$$L = N \pi D \quad (6)$$

So, the Sagnac phase shift can be rewritten as:

$$\Delta \phi = \frac{2\pi L D}{\lambda c} \Omega \quad (7)$$

As one example in a typical IFOG (200m coil length, 10cm-diameter coil) for measurement of the earth angular rotation ($\Omega = 15 \text{ }^\circ/\text{h} = 0.73 \text{ } \mu\text{r/s}$), the sensor detects a phase difference of $\Delta \Phi = 36 \text{ } \mu\text{r}$, corresponding to an optical path difference of the order of 10-12 m [9].

4. Closed-loop EF-FOG Configuration and Operation

In this structure the weak feedback signal is amplified by the Er-Doped Fiber Amplifier (EDFA) to prevent the laser scattering. Fiber amplifier is assumed to be linear, which means there are no gain effects. The output signal is the sum of interferometric CW and CCW beams in the total route. The modulator is located in sagnac loop. If the

phase modulator frequency is selected properly, the output signal will be a series of short pulses [8]. Hence modulation frequency of phase modulator and route delay must be approved by the equation:

$$\omega_m \tau = 2n\pi \quad (8)$$

Where ω_m is angular frequency of the phase modulation, and τ is the time delay in whole round trip loop consisting of Sagnac loop and amplified fiber optic loop. If the sharpness of output pulses could not be adjusted by phase modulation, by changing EDFA gain it can be compensated. If this equation $\omega_m \tau = 2n\pi + \phi_0$ is not realized, for example due to detuning, there will be a phase shift ϕ_0 that can be demodulated as an error signal for phase modulated (PM) technology. The operation of the FE-FOG is sensitive to the EDFA gain [10]. In theory the first interferometric output signal without feedback is equal to ordinary IFOG as:

$$P_1(t) = K_1 \left\{ 1 + v \cos \left[\phi_s + \phi_e \cos(\omega_m t) \right] \right\} \quad (9)$$

Where v is the interferometric coefficient and K_1 is a parameter that expresses the loss resulting from the Sagnac loop and the couplers of the Sagnac interferometer, ω_m is the modulation frequency, ϕ_e is the effective phase-modulation depth, which is expressed as

$$\phi_e = 2\phi_m \sin(\pi f_m \tau_s) \quad (10)$$

τ_s is the wave-propagation time through the Sagnac loop (please note the difference with the total time round-trip delay τ) and is expressed as $\tau_s = nL/c$ (where L is the length of Sagnac loop), and ϕ_m is the phase-modulation depth. ϕ_s is the Sagnac phase shift induced by rotational movement, which is expressed as Equation (7) in the previous section.

By considering the effect of optical feedback, the second-time interference signal experienced after the feedback has been derived is

$$P_2(t) = AK_1^2 K_2 \left\{ 1 + v \cos \left[\phi_s + \phi_e \cos(\omega_m t - \omega_m \tau) \right] \right\} \times \left\{ 1 + \cos \left[\phi_s + \phi_e \cos(\omega_m t) \right] \right\} \quad (11)$$

And the third-time interference signal that occurs after feedback has been twice derived is

$$\begin{aligned} P_3(t) = & A^2 (K_1^3 K_2^2)^2 \left\{ 1 + v \cos \left[\phi_s + \phi_e \cos(\omega_m t - 2\omega_m \tau) \right] \right\} \\ & \times \left\{ 1 + v \cos \left[\phi_s + \phi_e \cos(\omega_m t - \omega_m \tau) \right] \right\} \\ & \times \left\{ 1 + v \cos \left[\phi_s + \phi_e \cos(\omega_m t) \right] \right\} \end{aligned} \quad (12)$$

Where A is the gain of the fiber amplifier and K_2 is a parameter that depends on the coupling ratio of the feedback couplers and the transmission loss in the feedback loop. For simplicity, we assume that $K = K_1 \cdot K_2$. The total output at the photodetector is the summation of the number of above-mentioned interferences and is expressed as

$$P_{total}(t) = P_1(t) + P_2(t) + P_3(t) + \dots, \quad (13)$$

If $\omega_m \tau = 2n\pi$, the total photodetector output can be realized by proper adjustment of the modulation frequency to match the round-trip time, and we can have:

$$P_{total}(t) = \frac{K \{1 + v \cos [\phi_s + \phi_e \cos(\omega_m t)]\}}{1 - AK \{1 + [\phi_s + \phi_e \cos(\omega_m t)]\}} \quad (14)$$

Where K is the photodetector coefficient, because the total output is a series of short pulses, we can determine the peak value through the following equation:

$$\begin{aligned} P'_{total}(t) &= 0 \\ Kv \sin [\phi_s + \phi_e \cos(\omega_m t)] &= 0 \\ [\phi_s + \phi_e \cos(\omega_m t)] &= 2n\pi, \quad n=0,1,2,3, \dots \end{aligned} \quad (15)$$

Above Equation is a condition required to find the peak position of the output pulse that is valid for both cases of rotation and nonrotation, please note that only those equations of even π correspond to the peak position. From this equation and condition we can see that the output pulse shifts if rotation occurs.

For Closed-Loop FE-FOG In Eq.(10) if ϕ_e is selected to be between $0 < \phi_e < 2\pi$ and $\phi_s = 0$ there is no rotation, Eq.(10) is satisfied only when $n=0$. In this case, the peak positions of the output pulse are determined through the following equation:

$$\omega_m t_0 = \frac{2i+1}{2} \pi, \quad i=0,1,2, \dots \quad (16)$$

Here t_0 represents the peak positions corresponding to the nonrotation case and i denotes the peak number of the output pulse in the time axis. We see that the peak positions are not affected by the phase-modulation depth ϕ_e when there is no rotation. On the other hand, when rotation occurs ($\phi_s \neq 0$) the peak positions are affected by the Sagnac phase shift and can be determined by:

$$\omega_m t_r = \arccos \left(\frac{\phi_s}{\phi_e} \right) + 2i\pi, \quad i=0,1,2, \dots \quad (17)$$

Where t_r denotes the peak positions when rotation occurs and i has the same meaning as in Eq. 16. Comparing Eqs. 16 and 17, we see that the peak positions shift if rotation occurs, and the shift of the peaks is just equal to $\Delta t = t_r - t_0$. Therefore, the peak positions are influenced by only the Sagnac phase shift if rotation occurs and if we fix the phase-modulation depth ϕ_e . We can thus determine the rotation rate by the detection of the peak shift Δt of the output pulse.

In this paper the wave-length of optical source is $\lambda_0 = 1.5 \mu m$, the modulation frequency of the phase modulator, $f_m = 0.209790 \text{ MHz}$ ($\omega_m = 2\pi \cdot f_m$), and the radius of the Sagnac loop is $R = 0.05m$. The round-trip length is 500 m, which is selected to match

the modulation frequency for the pulse output, of which the Sagnac-loop length is 460 m and the length of the EDFA (including the pigtail of couplers) is 40 m. The interferometric coefficient is $\nu=0.96$, the photodetection coefficient is $K=0.2$, the parameter $K' = 0.06$, the effective phase-modulation depth is $\phi_e = 0.6 \text{ rad}$, and the Sagnac phase shift is $\phi_s = 0$ for the nonrotation case.

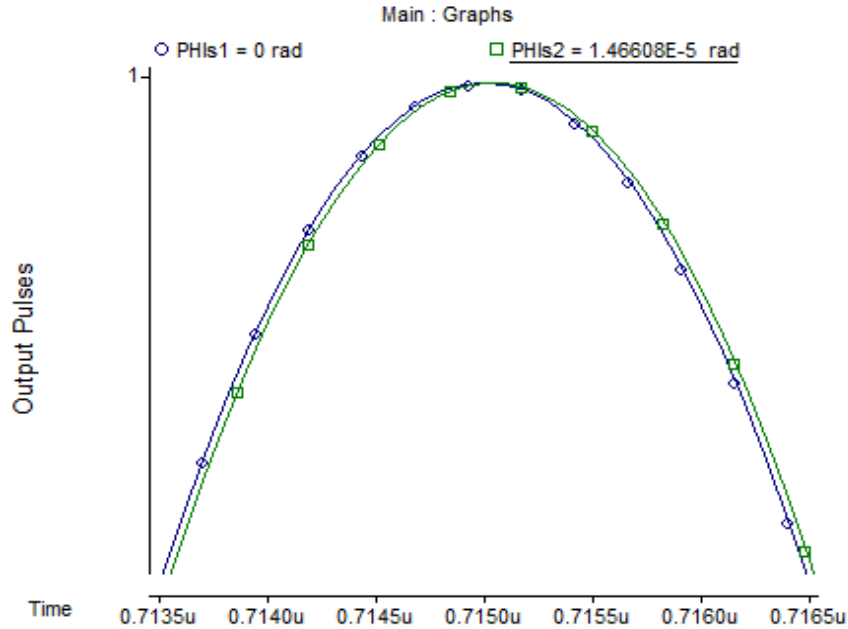


Figure 1. Rotation Measurement for Closed-loop EF-IFOG $\Delta t = 3.70741 \times 10^{-11}$

Figure 1 demonstrates the principle of the rotation measurement for the Closed-loop EF-IFOG method when the output pulse is shifted by rotation. The plots are normalized and $\phi_e = 0.18 \text{ rad}$. We see that the peak position shifts if rotation occurs, phase shift $0^\circ/h$ and $3.6^\circ/h$. Further calculations show that the shift is increased as the rotation rate increases. The very sharp peak of the output pulse can result in a high-resolution rotation measurement. From Eqs. 7 and 15–17 (in Eq. 16, $i=0,2,4$), we can derive the rotation rate as:

$$\Omega = -\frac{\lambda_0 c}{4\pi RL} \phi_e \cos(\omega_m t_0 + \omega_m \Delta t) = \frac{\lambda_0 c}{4\pi RL} \phi_e \sin(\omega_m \Delta t) \quad (18)$$

Where Δt is the time shift of the output peak as a result of the rotation, In Closed-Loop Method for the FE-FOG, we selected ϕ_e with a condition of $2\pi < \phi_e < 4\pi$. In such a case the output pulse is shifted by only the rotation. In this section, we hope to show that the output pulse is affected by both rotation and phase modulation, so that we can use the phase modulation to compensate the Sagnac phase shift. Such a technical idea is consistent with the closed-loop method.

In Eq. (15), if we assume that $\phi_s = 0$ (nonrotation) and we select $2\pi < \phi_e < 4\pi$, e.g., $\phi_e = 2.2\pi$, then Eq. (15), can be satisfied by $n=1$, $n=0$, and $n=-1$, which means that the output pulse has three kinds of peaks. The peaks corresponding to $n=0$ have the same properties as do those of the open-loop method and will not be affected by the phase modulation; however, the peaks corresponding to $n=1$ or $n=-1$ will be in fenced by both

the Sagnac phase shift and the phase-modulation depth. This performance can be used for the rotation measurement.

Figure 2 shows comparison of output pulses for different phase modulation.

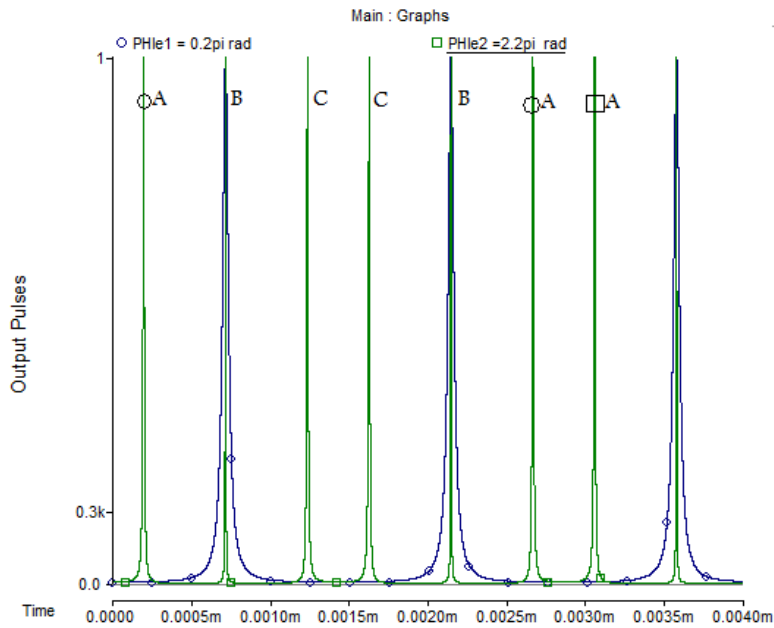


Figure 2. The Comparison of the Output Pulses for Different Phase Modulations when One Value of ϕ_e , $0 < \phi_e < 2\pi$ and $2\pi < \phi_e < 4\pi$. The Plots are Normalized

Figure 2 shows that the output pulses related to $\phi_e = 0.2\pi$ is simple, but, the output pulses related to $\phi_e = 2.2\pi$ are complicated and consist of three kinds of peaks

designated A, B, and C. (Note: if we select ϕ_e to be greater than 4π , even more output peaks will appear, because in Eq. (15) n also includes integers over. This case can also be analyzed similarly). The peak positions for A, B, and C are determined by $n = 1, 0, -1$, respectively, in Eq. (15). In this paper, we look at the peak positions corresponding to peaks A (peaks C also have similar properties). In one time period, peaks A also consist of two additional peaks, marked with circles and squares, whose positions are determined by:

$$\begin{aligned} \omega_m t_A &= \arccos(2\pi / \phi_e) + 2n\pi \\ \omega_m t_A &= 2\pi - \arccos(2\pi / \phi_e) + 2n\pi, n=0,1,2, \dots \end{aligned} \quad (19)$$

$n=0,1,2, \dots$ respectively. If the Sagnac phase shift induced by rotation is canceled by the phase modulation of the phase modulator, the peak positions corresponding to peaks A will not shift in spite of rotation's occurring. To realize this phase compensation we can feed back an electrical signal at the phase modulator. The rotation rate can thus be evaluated through the value of the phase modulation. Further calculations also show that, although in the closed-loop case (when both rotation and feedback control of ϕ_e occur) peaks B and C are shifted, they cannot cross with peaks A. This is because, for in any case, the peak positions of peaks A, B, and C are determined from Eq. (15) with $n = 1, 0,$

-1, respectively, and they always have different values. The above result tells us that in the closed-loop case the dynamic range is large.

A more detailed mathematical description is presented in the following paragraphs.

We first consider the case of nonrotation ($\phi_s = 0$), for which the peak positions corresponding to peaks A can be determined by

$$\phi_{e0} \cos(\omega_m t_A) = 2\pi \quad (20)$$

Where ϕ_{e0} is the phase-modulation depth corresponding to the nonrotation case, on the other hand, when rotation occurs and if the electrical-feedback signal is placed on the phase modulator, the peak positions corresponding to peaks A will not change, and then we have:

$$\phi_s = 2\pi - (\phi_{e0} + \delta\phi_e) \cos(\omega_m t_A), \quad (21)$$

From Eqs. (20) and (21) we can further derive

$$\phi_s = -\delta\phi_e \cos(\omega_m t_A) = -2\pi \frac{\delta\phi_e}{\phi_{e0}}, \quad (22)$$

We can evaluate the rotation rate by detecting $\delta\phi_e$.

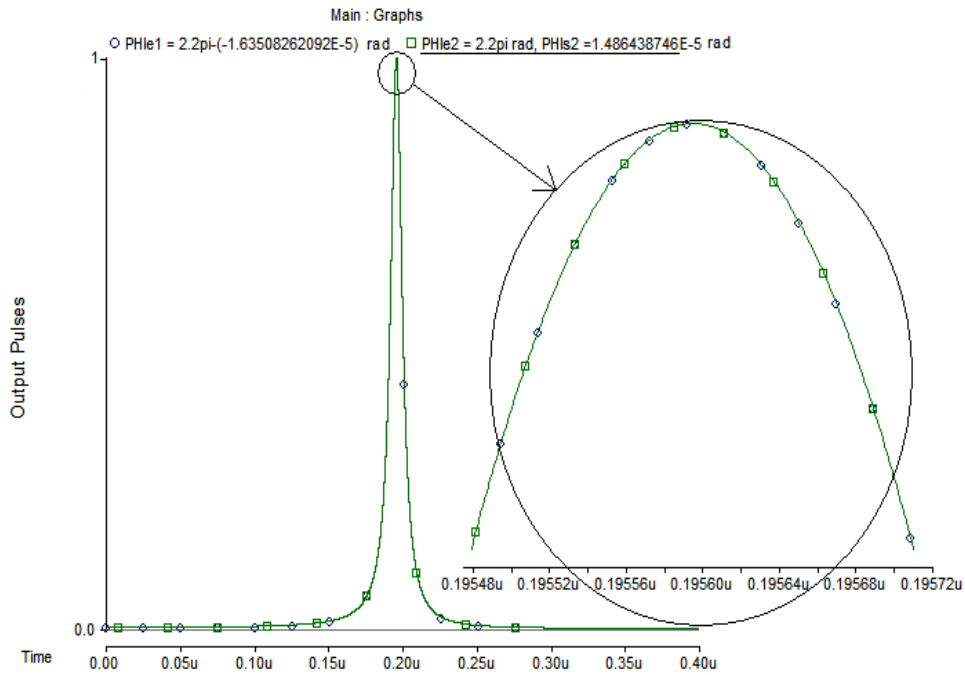


Figure 3a. Output Pulse when the Rotation doesn't Exist $\Omega = 0$ and

$$\phi_e = \phi_{e0} = 2.2\pi$$

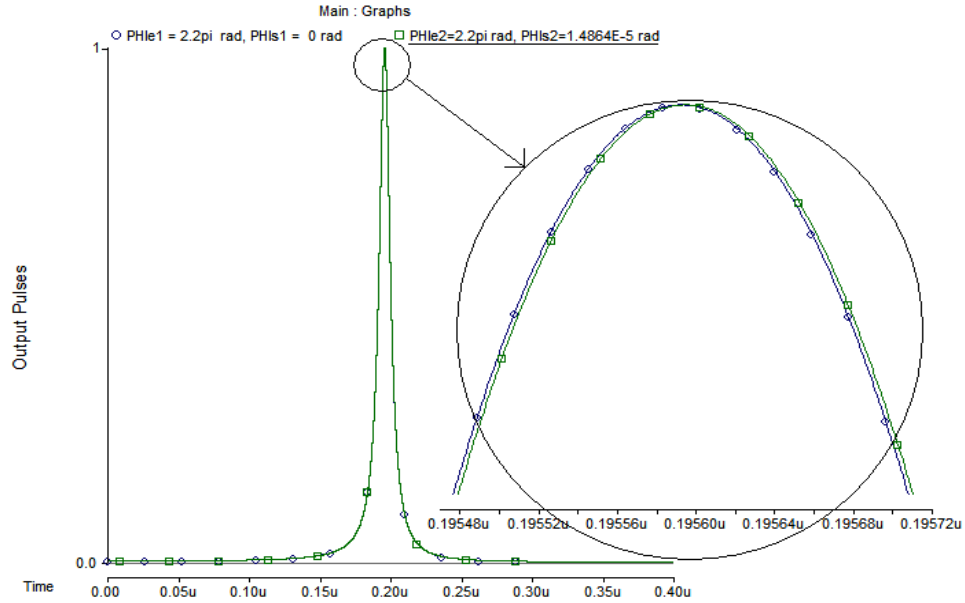


Figure 3b. Output Pulse when Rotate without Electric Feedback Signal in Phase Modulator $\Omega = 3.65^\circ / h$ and $\phi_e = \phi_{e0} = 2.2\pi$

Figure 3 shows the variation of the phase-modulation depth $\delta\phi_e$ as a function of the rotation rate for the closed loop. Figure 5a shows the output pulse when the rotation doesn't exist $\Omega = 0$ and $\phi_e = \phi_{e0} = 2.2\pi$ and Figure 5b shows the output pulse when rotate without electric feedback signal in phase modulator $\Omega = 3.65^\circ / h$ and $\phi_e = \phi_{e0} = 2.2\pi$ therefore when rotation occur output pulses shifted. We can see the peak that shifted by rotation could back to the first position that $\delta\phi_e$ shows the variation of phase modulation induced by electric feedback, that means the rotation rate of $\Omega = 3.65^\circ / h$ needs the phase compensation $\delta\phi_e = -1.63508262 \times 10^{-5}$.

5. Conclusion

In this paper, a comprehensive formulation of Closed-loop interferometric fiber optic gyroscope, so called EF-FOG was studied. The functionality of the closed-loop fiber-optic gyroscope EF-FOG, based on multiple utilizations of the Sagnac loop and amplified optical feedback, has been proposed and theoretically investigated. The new gyroscope is termed as feedback Er-doped fiber-optic amplifier (FEDFA). A low-coherence light source is used in this FOG [11]. Amplification of a weak feedback gyroscope signal is performed by the incorporated EDFA. The final gyroscope output is pulsed if the modulation frequency of the phase modulator matches the round-trip time [12]. Sagnac phase shift can induce a shift of the output pulse, which is used for the rotation measurement.

References

- [1] M. Merlo, N. Orgia and S. Donati, "Fiber Gyroscope Principles", Handbook of Fibre Optic Sensing Technology, John Wiley & Sons, Ltd. Chapter 16, (2000), pp. 1-23.
- [2] H. C. Lefevre, "Fundamentals of the Interferometric Fiber-Optic gyroscope", Optical review, vol.4, no. 1a, (1997), pp. 20-27.
- [3] S. Oho, H. Kajioaka, and T. Sasayama, "Optical Fiber Gyroscope for Automotive Navigation", IEEE transactions on vehicular technology, vol. 44. no. 3, (1995), pp. 698-705.

- [4] K. Shaikh, R. Shariff, F. Nagi, H. Jamaluddin, and S. Mansor, "Inertial Navigation Sensors; Data Processing and Integration With GPS For Mobile Mapping", (2005).
- [5] M. R. Nasiri-Avanaki, V. Soleimani and R. Mazrae Khoshki "Comparative Assessment on the performance of Open-loop and Closed-loop IFOGs", Optics and Photonics Journal, vol.2 no.1, (2012), pp. 17-29.
- [6] S. M. Bennett, S. Emge and R. B. Dyott, "Fiber Optic Gyroscopes for Vehicle Use", Intelligent Transportation System, ITSC, IEEE Conference, (1998), pp. 1053-1057.
- [7] R. M. Khoshki, "Analysis of Closed-Loop Interferometric Fiber Optic Gyroscope (EF-FOG) and implementation", M.Sc. Thesis, Razi University, (2009).
- [8] C. X. Shi, T. Yuhara, H. Iizuka, and H. Kajioaka, "New interferometric fiber-optic gyroscope with amplified optical feedback", Applied Optics, vol.35, no.3, (1996).
- [9] R. Y. Liu and G. W. Adams, "Interferometric Fiber Optic Gyroscope: A Summary of Progress", IEEE conference Las Vegas, USA (1990), pp. 31-35.
- [10] C.-Y. Liaw, Y. Zhou, Y.-L. Lam, member IEEE Characterization of an Open-Loop Interferometric Fiber-Optic Gyroscope with the Sagnac Coil Closed by an Erbium-Doped Fiber Amplifier. Lightwave Technology, Journal, vol. 16, no. 12 , (1998).
- [11] A. Nouredin, M. Mintchev, D. Irvine-Halliday and H. Tabler, "Computer Modelling of Microelectronic Closed Loop Fiber Optic Gyroscope," IEEE Canadian Conference on Electrical and Computer Engineering, Edmonton, 9-12, (1999), pp. 633-638.
- [12] B. Se'men, "Simulation on Interferometric Fiber Optic Gyroscope with Amplified Optical Feedback," Middle East Technical University (METU), (2003).

Authors



Rohollah Mazrae Khoshki, PhD student in Oakland University, Rochester, MI, USA, in Embedded System Electrical Eng., He is working as a teaching assistant for the electrical and computer engineering department at Oakland University. He investigated and designed of Interferometric Fiber Optic Gyroscope (IFOG) as his Master Thesis, designed and implemented of Heater Health Monitoring (HHM) project for Nextthermal Company. He is interested in Embedded Systems, FPGAs and Microcontrollers, Robotics and control, Image processing and Optoelectronic in research and practical applications.



Dr. Subramaniam Ganesan, Professor of Electrical and Computer Engineering, Oakland University, Rochester, MI, 48309, USA. He has over 25 years of teaching and research experience in Digital systems. He served as the chair of the CSE department from 1991 to 98. He is with Electrical and Computer Engineering Department since 2008. He received his masters and Ph.D. from Indian Institute of Science (IISc) Bangalore, India. He worked at National Aeronautical Laboratory (NAL) India, Ruhr University, Germany, Concordia University Canada, and Western Michigan University before joining Oakland University in 1986.